

Published in final edited form as:

Nat Microbiol. 2019 November 01; 4(11): 2001–2009. doi:10.1038/s41564-019-0525-3.

## Shigella-mediated oxygen depletion is essential for intestinal mucosa colonization

Jean-Yves Tinevez<sup>#1,2</sup>, Ellen T Arena<sup>#3,4,€</sup>, Mark C Anderson<sup>3,4</sup>, Giulia Nigro<sup>3,4</sup>, Louise Injarabian<sup>3,5</sup>, Antonin C André<sup>3,5</sup>, Mariana Ferrari<sup>3,4</sup>, François-Xavier Campbell-Valois<sup>3,4,£</sup>, Anne Devin<sup>5</sup>, Spencer L Shorte<sup>1,6</sup>, Philippe J Sansonetti<sup>3,4,7</sup>, Benoit S Marteyn<sup>3,4,5,\*</sup>

<sup>1</sup>UTechS PBI (Imagopole), C2RT, Institut Pasteur, Paris, France

<sup>2</sup>Image Analysis Hub, C2RT, Institut Pasteur, Paris, France

<sup>3</sup>Unité de Pathogénie Microbienne Moléculaire, Institut Pasteur, Paris, France

<sup>4</sup>INSERM Unité 1202, Paris, France

<sup>5</sup>Université Bordeaux, IBGC, CNRS UMR 5095, Bordeaux, France

<sup>6</sup>Institut Pasteur Korea, Scientific Direction, 16, Daewangpangyo-ro 712 beon-gil Bundang-gu, Seongnam-si, Gyeonggi-do, 13488 Rep. of Korea

<sup>7</sup>Collège de France, Paris, France

# These authors contributed equally to this work.

### Abstract

Pathogenic enterobacteria face various oxygen (O<sub>2</sub>) levels during intestinal colonization from the O<sub>2</sub>-deprived lumen to oxygenated tissues. Using *Shigella flexneri* as a model, we had previously demonstrated that epithelium invasion is promoted by O<sub>2</sub> in a Type III secretion system (T3SS)-dependent manner<sup>1</sup>. However, subsequent pathogen adaptation to tissue oxygenation modulation remained unknown. Assessing single-cell distribution, together with tissue oxygenation, we demonstrate here that the colonic mucosa O<sub>2</sub> is actively depleted by *Shigella flexneri* aerobic respiration, not host neutrophils, during infection, leading to the formation of hypoxic foci of infection. This process is promoted by T3SS inactivation in infected tissues, favoring colonizers over explorers. We identify the molecular mechanisms supporting infectious hypoxia induction,

Users may view, print, copy, and download text and data-mine the content in such documents, for the purposes of academic research, subject always to the full Conditions of use:[http://www.nature.com/authors/editorial\\_policies/license.html#terms](http://www.nature.com/authors/editorial_policies/license.html#terms)

\*Corresponding author: Benoit Marteyn (marteyn@pasteur.fr), Institut Pasteur, Unité PMM, Paris, France; Phone +33 1 45488308; Fax +33 1 45488953.

€Current affiliation: Laboratory for Optical and Computational Instrumentation (LOCI), University of Wisconsin - Madison, 1675 Observatory Drive, Madison, WI 53706, USA

£Current affiliation: University of Ottawa, Faculty of Science, Department of Chemistry and Biomolecular Sciences and Faculty of Medicine, Department of Biochemistry, Microbiology and Immunology, Ottawa, Ontario, Canada

#### Competing interest statement

The authors declare no competing interests

#### Author contributions

BSM, JYT and ETA designed the experiments, interpreted the data, and wrote the paper. MA designed *Shigella* mutants. GN, LI, AA, MF and FXCV contributed to their study *in vitro* and *in vivo*. JYT conducted quantitative analysis of the data. AD, SLS and PSJ contributed to data interpretation.

and we demonstrate here how enteropathogens optimize their colonization capacity in relation to their ability to manipulate tissue oxygenation during infection.

Pathogenic enterobacteria virulence and first-line immune cells', particularly neutrophils', survival and function are highly modulated by oxygen (O<sub>2</sub>)<sup>1,2,3,4</sup>. Most virulent enterobacteria (*Shigella* spp., *Listeria* spp., *Salmonella* spp., pathogenic *E. coli*, or *Yersinia pestis*) are well adapted to these changing microenvironments<sup>5</sup>, suggesting adaptability to various O<sub>2</sub> levels represents a selective advantage crucial for their infectious capacity. The colonization process involves three key steps: degradation of the mucus layer, invasion of the epithelium mediated by the T3SS, and formation of primary foci of infection. We previously demonstrated that *S. flexneri* T3SS activation requires O<sub>2</sub>, which diffuses on the epithelium surface<sup>1</sup>. However, tissue oxygenation modulation during the dissemination of enteropathogens and its impact on colonization or immune response efficiency remains largely unknown, although hypoxia has been previously reported in a TNBS colitis model of inflammation<sup>6</sup>.

In this work, we show that oxygen is depleted during tissue colonization by enteropathogens, using *S. flexneri* as a model, leading to the formation of hypoxic foci of infection. We designed a quantitative image analysis method allowing the assessment of tissue oxygenation at a single-cell level for both bacteria and neutrophils. We demonstrate that *S. flexneri* aerobic respiration is essential for O<sub>2</sub> depletion within the colonic mucosa, not neutrophils, as previously demonstrated in a non-infectious model of inflammation<sup>7</sup>. We show that formation of hypoxic foci of infection is the primary *S. flexneri* colonization strategy, which is promoted by the repression of T3SS activity. Our results demonstrate that the interaction between *S. flexneri* and immune cells occurs mainly in the absence of O<sub>2</sub>. We anticipate our results will have a significant impact on new vaccine and antibiotic development strategies, as well as reappraisal of immune response and host-pathogen interactions in low O<sub>2</sub> conditions.

We recently observed that hypoxia was induced within the colonic mucosa upon *S. flexneri* infection<sup>8</sup> using a hypoxia reporter, EF5<sup>9</sup>. Here, measuring relative hypoxia levels from the epithelial surface to the submucosa (Supplementary Table 1), we confirmed this preliminary observation (Figure 1a) and demonstrated that during infection, compared to basal conditions, the degree of hypoxia increased significantly to a depth of 130 μm (Figure 1b, *p* < 0.05). In basal conditions, the 'physiological hypoxic status' of the epithelium was confirmed, as previously reported in the mouse<sup>6,7</sup> (Figure 1b, uninfected tissues).

Taking into account the potential heterogeneity of the bacteria population<sup>10</sup>, we developed a quantitative imaging strategy at a single-bacteria level, as previously reported<sup>11</sup>, to localize individual bacteria and assess hypoxia levels (Figure 1c and Supplementary Figure 1a-c). First, we revealed that most bacteria (99.71%, Supplementary Figure 1a) were located within foci of infection formed in the colonic extracellular matrix ('clustered' bacteria, defined as having at least 6 neighboring bacteria within 16 μm) not dispersed within the mucosa ('dispersed' bacteria, defined as having a closest neighboring bacteria beyond 30 μm, Figure 1c and Supplementary Figure 1a). We demonstrated that *S. flexneri* faced hypoxic conditions specifically within foci of infection, not when dispersed elsewhere in the

mucosa (Figure 1d-f,  $p < 10^{-10}$ ). This result implies that *S. flexneri* adaptation to low- $O_2$  levels is crucial for tissue colonization. We demonstrated that a *S. flexneri* *fnr* mutant strain (FNR, which mediates the adaptation of *S. flexneri* to anaerobiosis<sup>1</sup>) did not propagate within foci of infection and was avirulent (Supplementary Figure 2a), as previously demonstrated<sup>1</sup>; also, the neutrophil population was reduced, a sign of limited inflammation (Supplementary Figure 2a). In a rabbit ileal loop model, we confirmed that FNR was specifically required for *S. flexneri* propagation in an inflammatory environment, but not mandatory for its fitness within the intestinal lumen (Supplementary Figure 2b).

Neutrophils represent the most abundant immune cell population recruited upon *Shigella* infection, and their activation has been previously identified as responsible for hypoxia induction in a TNBS colitis model of inflammation<sup>7</sup>. Neutrophils were specifically labeled with MUB<sub>40</sub>, (or Myelotracker, a neutrophil lactoferrin marker<sup>12</sup>), allowing single-cell analyses (Figure 1g). We observed that neutrophils were in closest proximity to ‘clustered’ bacteria compared to ‘dispersed’ bacteria (Figure 1h) and that the level of hypoxia quantified at a single-neutrophil level was significantly higher when located in the vicinity of ‘clustered’ bacteria (Figure 1i). Hypoxia levels measured at a single-bacteria level around ‘clustered’ and ‘dispersed’ *S. flexneri* remained similar in conventional and neutropenic animals (Figure 2a-b), suggesting that neutrophil contribution is not an essential factor for hypoxia induction. As expected, a significantly reduced amount of neutrophils were detected in the infected colonic mucosa of neutropenic animals; the *S. flexneri* population was only mildly reduced (Supplementary Figure 2c). Neutrophil hypoxia levels were compared to the closest bacteria hypoxia profiles; for more than 95% of neutrophils, hypoxia levels were not found to be significantly higher than the hypoxia generated by bacteria in their vicinity (Supplementary Figure 2d).

Since neutrophils’ contribution seemed limited,  $O_2$  consumption mediated by *S. flexneri* was investigated as a potential cause of local  $O_2$  depletion observed within foci of infection. *S. flexneri* population density in foci was estimated from confocal images to be  $3.9 \cdot 10^9 \pm 2.7 \cdot 10^9$  cell/mL for ‘clustered’ bacteria, compared to  $1.3 \cdot 10^6 \pm 1.1 \cdot 10^6$  cell/mL for bacteria ‘dispersed’ in the tissue (Figure 2c-d). The impact of bacterial density on *S. flexneri*  $O_2$  consumption kinetics was then assessed *in vitro* using a dedicated device allowing the inoculation of bacteria in a sealed anoxic tube containing culture medium stabilized at 40 mmHg  $O_2$ , reflecting estimated physiological  $O_2$  levels<sup>13</sup> (Figure 2e).  $O_2$  consumption rate was correlated to the *S. flexneri* population cell density (Figure 2f). At a cell density measured within foci of infection (between  $1.1 \cdot 10^9$  and  $5 \cdot 10^9$  cell/mL), complete  $O_2$  depletion by *S. flexneri* occurred rapidly ( $t_{anoxia} = 2.3 \pm 1.1$  min, Figure 2f); similar results were obtained with other pathogenic enterobacteria, including *E. coli*, *S. typhimurium*, *L. monocytogenes*, and *Y. pestis*, though not with *Lactobacillus casei*, an aerotolerant anaerobe (Supplementary Figure 3). When a similar experiment was conducted at a density corresponding to the ‘dispersed’ population, complete  $O_2$  depletion was not achieved over the measurement period (Figure 2f). The co-incubation of neutrophils with *S. flexneri* at a pathophysiological cell density ( $8.1 \cdot 10^7 \pm 5.4 \cdot 10^7$  cell/mL, Figure 2d) had no impact on the timing of complete  $O_2$  depletion compared to *S. flexneri* alone (clustered,  $t_{anoxia} = 2.4 \pm 1.0$  min,  $p > 0.05$ , Figure 2g). A mild increase of  $O_2$  consumption was observed when co-incubating neutrophils with *S. flexneri* at a cell density corresponding to the ‘dispersed’

population or heat-killed bacteria ( $t = 10$  min,  $p < 0.01$  and  $p < 0.05$ , respectively), although complete O<sub>2</sub> depletion was not achieved over the measurement period (Figure 2g). We demonstrate here that O<sub>2</sub> depletion during infection seems driven by *S. flexneri*, while neutrophils contribute comparatively much less.

We reasoned that *S. flexneri* aerobic respiration is responsible for the O<sub>2</sub> depletion observed *in vivo*. At the end of the aerobic respiratory chain, O<sub>2</sub> is reduced to H<sub>2</sub>O by terminal cytochrome oxidases<sup>14</sup>: *S. flexneri* expresses two cytochrome oxidases named *bd-I* (CydAB) and *bd-II* (AppCB), similarly to *E. coli*, (*S. flexneri cyoAB* genes are truncated) (Figure 3a). Therefore, we engineered *S. flexneri cydAB* and *appCB* mutants and noted that their cellular morphologies were indiscernible from the wild-type (Supplementary Figure 4a).

We showed that the *bd-I* complex (CydAB), but not the *bd-II* complex (AppCB), was essential for *S. flexneri*'s ability to consume O<sub>2</sub> (Figure 3b). Consistently, cytochromes *b* and *d* expressed by *S. flexneri* belong mainly to the *bd-I* complex (Supplementary Figure 4b), and *S. flexneri cydAB* displayed a growth defect in the presence of O<sub>2</sub> compared to the wild-type strain, confirming that aerobic respiration is defective in this mutant (Supplementary Figure 4c). The *S. flexneri cydAB (bd-I)* mutant was not virulent *in vivo*, O<sub>2</sub> depletion was not observed, and foci of infection were not formed in the colonic mucosa (Figure 3c-d); although it remained invasive and was phagocytized by neutrophils as per the wild-type strain *in vitro* (Supplementary Figure 4d). Consistent with previous results (Figure 2f-g), the co-incubation of neutrophils (with or without DPI, a neutrophil NADPH oxidase inhibitor) with *S. flexneri appCB (bd-II)* had no impact on timing of anoxia induction (Supplementary Figure 4e). When similar experiments were conducted with *S. flexneri cydAB* or upon activation with N-Formyl-Met-Leu-Phe (FmlF), a mild increase of oxygen consumption was observed and abolished by DPI (Supplementary Figure 4e,  $p < 0.05$ ); although anoxia was not reached in both conditions over the measurement period.

We confirmed that GLUT-1, a hypoxia-induced glucose transporter<sup>7</sup>, was overexpressed in non-infected epithelial cells (physiological hypoxia), but also within *S. flexneri* foci of infection (Figure 3f and Supplementary Figure 5a) though not upon *S. flexneri cydAB* mutant infection (Supplementary Figure 5a). To confirm that *S. flexneri cydAB* avirulence was caused by its defect in O<sub>2</sub> consumption, we co-infected guinea pigs with *S. flexneri* pGFP wild-type and *cydAB* pDsRed mutant strains. We confirmed that hypoxia was induced within foci of infection (GLUT-1 stabilization, Figure 3f), mediated by *S. flexneri* wild-type strain, and we demonstrated that, in this context, the *S. flexneri cydAB* mutant was able to colonize the colonic mucosa together with the wild-type strain (Figure 3f and Supplementary Figure 5b). The relative amount of *S. flexneri* wild-type and *cydAB* mutant strains in the lumen (comparing plasmid-cured BS176 and BS176 *cydAB* mutant strains, Figure 3f and Supplementary Figure 5b) or within the colonic mucosa (comparing M90T and M90T *cydAB* mutant strains, Figure 3f and Supplementary Figure 5b) was similar (Competitive Index value around 1), as observed *in vitro* under anoxic conditions (Figure 3g). We therefore confirmed our hypothesis that *S. flexneri* aerobic respiration was the primary cause of hypoxia induction *in vivo*, explaining its essential role for tissue colonization<sup>15</sup>. The ability of *S. flexneri* to grow in the absence of O<sub>2</sub> supports the expansion

of foci, whose formation appears to be the preferential strategy for tissue colonization (composed of 99.71% total bacteria, Supplementary Figure 1a).

We hypothesized that the repression of *S. flexneri*'s dissemination capacity may promote foci of infection extension by favoring colonizing over exploring bacteria. *S. flexneri*'s ability to invade host cells relies on the T3SS, whose activity is significantly reduced in hypoxic conditions<sup>1</sup>. To assess the level of T3SS activity of individual bacterium within colonic tissues, we measured the fluorescence signal produced by a *S. flexneri* strain harboring the pTSAR plasmid, which has a fast-maturing eGFP under the control of a T3SS activity-dependent promoter<sup>16</sup>.

The positive correlation between O<sub>2</sub> availability and the T3SS-activity in the presence of the secretion inducer Congo red (congo red, +CR) was confirmed *in vitro* (fast-maturing eGFP fluorescent signal and IpaB secretion, Figure 4a-b,  $p < 0.001$ ). We also previously confirmed oxygen-dependent type III secretion of effectors *in vitro* by western blot<sup>1</sup>. The activity of *S. flexneri* T3SS was also assessed *in vivo* within foci of infection (Figure 4c). Performing a single-bacteria analysis, we demonstrated that *S. flexneri* T3SS was mostly inactive in infected tissues (87.55% total bacteria, Figure 4d-e,  $n = 265$  bacteria). These results confirm that hypoxic conditions encountered in foci of infection blocks T3SS activation, hence limiting *S. flexneri* dissemination to adjacent host cells and promoting tissue colonization through foci expansion.

Here we show that intestinal mucosa colonization by *S. flexneri* occurs through the formation and expansion of hypoxic foci of infection. In summary, while O<sub>2</sub> is essential for *S. flexneri* T3SS-dependent epithelium invasion<sup>1</sup>, its depletion is conversely mandatory for subsequent tissue colonization. The ability of *S. flexneri* to survive this low-oxygenated environment, as well as the associated blockade of the T3SS, contributes to the expansion of foci of infection.

Our results reveal that the adaptation of invasive pathogens to various O<sub>2</sub> levels is essential for tissue colonization. In fact, to our knowledge, pathogenic microorganisms that are not facultative anaerobes are not invasive. We demonstrate that O<sub>2</sub> depletion by pathogenic enterobacteria may be considered a community behavior<sup>17</sup>, querying previous concepts such as the O<sub>2</sub> availability in colonic inflammation models and bacteria adaptation to these pathophysiological environments<sup>18</sup>. In particular, improved methods will be required to study the population heterogeneity within foci in regards to O<sub>2</sub> levels. For example, more than 40% of individual bacteria were neither 'clustered' nor 'dispersed' in neutropenic animals (Supplementary Table 1), highlighting the importance of foci formation in response to neutrophil recruitment and antimicrobial activity.

O<sub>2</sub> depletion by pathogenic enterobacteria is expected to modulate the survival and function of immune cells<sup>19,20</sup>, particularly neutrophils<sup>2,3,4</sup>; important O<sub>2</sub>-dependent antimicrobial functions, such as ROS production, are likely to be altered. The contribution of alternative electron transfer machineries for oxygen-depletion and enteropathogen virulence, such as the recently described *Listeria monocytogenes* extracellular electron transport (EET)<sup>21</sup>, requires further investigation. The respective contributions of enteropathogens, commensal

flora, and host cells (*i.e.* neutrophil activation, epithelial cell death, etc.) in oxygen depletion may be further investigated in other acute or chronic models of inflammation. In conclusion, this “battle to breathe” is anticipated to be crucial for the outcome of infection and will have to be taken into account in the development of truly effective antibiotics or vaccines targeting pathogens in low-O<sub>2</sub> environments for efficient clearance or protection.

## Material and Methods

### Bacterial strains, growth conditions

*Shigella flexneri* 5a (*Shigella*) strains (wild-type M90T, plasmid-cured BS176 M90T *fnr* mutant, and BS176 *fnr* mutant) and *Staphylococcus aureus* were propagated in Trypticase soy media (TCS, Oxoid) or on TCS plates, supplemented with Congo Red (0.01%, Sigma) for *Shigella* strains. *Escherichia coli*, *Salmonella typhimurium*, and *Listeria monocytogenes* were cultured in Luria Bertani (LB) medium. *Lactobacillus casei* was grown in deMan, Rogosa and Sharpe (MRS) broth (Sigma-Aldrich). *S. flexneri* M90T was used as a wild-type *Shigella* strain. Targeted deletion of *appCB* and *cydAB* genes was performed using  $\lambda$  red recombination using the following primers *appCB*1 (5'-ATGTGGGATGTCATTGATTTATCGCGCTGGCAGTTTGTCTCCATATGAATATCCTCCTTAGTTCC-3') and *appCB*2 (5'-TTAGTACAACCTCGTTTTTGTACGGCGGAGAGTTTCTGTTGTGTAGGCTGGAGCTGCTTC-3') with plasmid pKD3 to generate a PCR product containing a chloramphenicol resistance cassette flanked on each end with 50bp corresponding to the *S. flexneri appCB* genes. Primers *cydAB*1 (5'-TTAGTACAGAGAGTGGGTGTTACGTTCAATATCTTCTTTGCATATGAATATCCTCCTTAGTTCC-3') and *cydAB*2 (5'-ATGTTAGATATAGTCGAACTGTCGCGCTTACAGTTTGCCTGTGTAGGCTGGAGCTGCTTC-3') were used with plasmid pKD4 to generate a PCR product containing a kanamycin resistance cassette flanked on each end with 50bp corresponding to the *S. flexneri cydAB* genes. KO generation was performed under anoxic conditions to limit potential toxicity from inactivating the respiratory pathway. Isolated mutants were passaged on TSA plates containing 0.01% congo red to confirm virulence plasmid maintenance.

*Shigella flexneri* 5a fluorescent strains (wild-type M90T, M90T *cydAB*, plasmid-cured BS176, BS176 *cydAB*, M90T *fnr* mutant, and BS176 *fnr* mutant) were generated by transforming the pFPV25.1 (AmpR) or pDsRed (AmpR) plasmids, as indicated. Antibiotics were added as necessary at the following concentrations: chloramphenicol, 50  $\mu$ g/mL; ampicillin, 100  $\mu$ g/mL; kanamycin 50  $\mu$ g/mL. Experiments under different oxygen (O<sub>2</sub>) concentrations were performed in an anaerobic cabinet (Don Whitley DG250) or in a cabinet in which O<sub>2</sub> tensions can be controlled (Don Whitley H35 Hypoxystation).

To assess the level of the T3SS activity, *S. flexneri* 5a was transformed with pTSAR<sup>16</sup>, allowing the constitutive expression of CFP (cyan) and inducible expression of the fast maturing eGFP (dependent of the T3SS activity).

## Cytochrome quantification

The cellular content of cytochromes *b* and *d* hemes were calculated as described by Dejean et al.<sup>22</sup>, taking into account the respective molar extinction coefficient values (18.0  $\text{kM}^{-1}\text{cm}^{-1}$  and 27.9  $\text{kM}^{-1}\text{cm}^{-1}$ , respectively) and the reduced minus oxidized spectra recorded using a dual beam spectrophotometer (Aminco DW2000). Briefly, *S. flexneri* wt, *cydAB*, and *appCB* mutants strains were grown until  $\text{OD}_{600} = 2$  was reached. For each measurement, 100 OD units were centrifuged for 10 minutes at 5000 rpm, bacterial pellets were resuspended in distilled water ( $\text{dH}_2\text{O}$ ) up to 2 mL; 1 mL for the oxidized condition and 1 mL for the reduced condition (dithionite addition). The cytochrome maximum and minimum absorbance values were measured at 560 and 575, and 630 and 655 nm for cytochromes *b* and *d*, respectively, and expressed in mol/OD.

## Cell culture

**Blood collection, Neutrophils purification**—All participants gave written, informed consent in accordance with the Declaration of Helsinki principles. Peripheral Human blood was collected from healthy patients at the ICAReB service of the Institut Pasteur (authorization DC No.2008-68). Human blood was collected from the antecubital vein into tubes containing sodium citrate (3,8% final) as anticoagulant molecules. Guinea pig blood samples were collected on anesthetized animals by cardiac puncture.

Human or guinea pig neutrophils were purified as described previously<sup>23</sup>. Briefly, whole blood samples were centrifuged at 450x *g* for 15 min. Platelet rich plasma (PRP) was collected and centrifuged at 2500x *g* for 20 min to form platelet poor plasma (PPP). Blood cells were resuspended in NaCl 0.9% and dextran sulfate (0.72%). After 30 min sedimentation, the neutrophil-containing upper layer was centrifuged at 240x *g* for 10 min. The resuspended pellet was separated on a 2-layers Percoll (GE Healthcare) gradient (51%/42%) by centrifugation at 240x *g* for 20 min. Neutrophils were collected, and remaining red blood cells were removed using CD235a (glycophorin) microbeads (negative selection, Miltenyi Biotec).

For functional assays, human or guinea pig purified neutrophils were cultured in RPMI 1640 (Life Technologies) supplemented with 10 mM Hepes (Life Technologies).

**Epithelial cell culture**—The Hep2 cell line was purchased at the ATCC and was tested for mycoplasma contamination. Hep2 epithelial cells were cultured in a DMEM medium (ThermoFischer) supplemented with 10 % Fetal Calf Serum (ThermoFischer). For functional assays, Hep2 cells were incubated in DMEM medium supplemented with 10 mM Hepes, without FCS.

## Antibodies and fluorescent dyes

Hypoxia detection in guinea pigs was achieved by 2-nitroimidazole derivative EF5 molecule (University of Pennsylvania, USA) accumulation in tissues. An intracardiac injection (1.5 mL for 150 g guinea pig) of a 10 mM EF5 solution was performed one hour prior to *Shigella* challenge.

EF5 was immunodetected on fixed cells or tissues using an  $\alpha$ -EF5 antibody (ELK3-51) conjugated with a Cy3 fluorophore (ready-to-use solution, University of Pennsylvania, USA). Dapi (Invitrogen) was used at 1  $\mu\text{g}/\text{mL}$ . Neutrophils were labeled with the MUB<sub>40</sub>-Dylight405 marker<sup>12</sup>, binding to lactoferrin stored in specific and tertiary granules. GLUT-1 was detected with a mouse monoclonal antibody (Abcam, ab40084), used at 1:40 dilution and a secondary antibody conjugated with an Alexa647 fluorophore (ThermoFisher Scientific).

### **Bacterial cell infection *in vitro***

Cell entry assays, Hep2 epithelial cells were seeded (5.  $10^5$  cells/well) and grown overnight in 24-well tissue culture plates in indicated conditions (0, 5% and 21% O<sub>2</sub>). Neutrophils were directly seeded (5.  $10^5$  cells/well) in 24-well tissue culture plates. Cells were challenged at an MOI of 100 (Hep2) or 20 (neutrophils) with bacteria grown until the mid-log phase was reached in liquid culture under the same conditions. Bacteria were spun briefly onto cells by centrifugation at 2000x g for 10 min.

To measure bacterial entry, cells were challenged as above, incubated for 30 min at 37°C, after which gentamicin (50  $\mu\text{g}/\text{ml}$ ) was added for 30 min to kill extracellular bacteria. Cells were then washed three times with PBS, lysed with 1 mL 1% saponin in PBS, and bacteria recovered by plating to solid media. Results are expressed as the number of CFU/ml of cell lysate and are the average of at least three independent experiments performed in triplicate. Statistical significance was calculated using the Student's T-test.

### **In vitro O<sub>2</sub> quantification**

Gas proof glass tubes were first left in an anaerobic cabinet to remove all traces of exogenous oxygen and generate an anoxic atmosphere. The tubes were then filled with RPMI 1640 culture medium supplemented with 10 mM Hepes pre-stabilized at 37°C and pO<sub>2</sub> = 40 mmHg. Bacteria and neutrophils were prepared in similar conditions in adequate culture media and resuspended in the prepared glass tubes. Direct oxygen quantification was performed with a Clark-type sensor mounted with a needle (Unisense oximeter) over time and initiated immediately after bacteria or cell inoculation. Results are averaged from at least three independent experiments.

### **Animal models of shigellosis**

**Rabbit ligated ileal loop model**—Experiments on rabbits were approved by the Institut Pasteur local ethic committee (CETEA).

For evaluation of competitive indices, experiments were performed on independent occasions in at least two ileal loops in four animals in total. For competitive indices calculations, bacteria were grown in liquid media for three hours at 37°C, and a total  $10^7$  CFU of bacteria consisting of equal numbers of two or three strains in 500  $\mu\text{l}$  of physiological water were injected into loops. After an 18-hour infection, animals were sacrificed, and bacteria were recovered from the loops. Series of dilutions of the outputs were plated onto TCS plates containing antibiotics and congo red (CR), allowing the selection and counting of M90T (CR+ (red colony), Cm<sup>R</sup>, Km<sup>S</sup>), M90T *fnr* (CR+ (red



colony), Cm<sup>R</sup>, Km<sup>R</sup>), BS176 (CR- (white colony), Cm<sup>R</sup>, Km<sup>S</sup>), BS176 *fnr* (CR- (white colony), Cm<sup>R</sup>, Km<sup>R</sup>). The competitive index was calculated as the ratio of mutant to wild-type bacteria recovered from animals divided by the ratio in the inoculum; the results are the average of at least four samples originating from four different rabbits. For single strain infections (M90T, BS176, *fnr*, and BS176 *fnr*), 10<sup>7</sup> CFU were inoculated in ligated loops. After an 18-hour infection, animals were sacrificed and infected ileal loops collected. For immunohistochemistry, ileal loops were fixed in 4% buffered formalin, embedded in paraffin, and 5 µm sections obtained and stained with haematoxylin-eosin. *Shigella* strains were detected using a primary mouse anti-LPS antibody and an HRP-conjugated anti-mouse antibody (Dako).

**Guinea pig intrarectal infection**—Experiments on guinea pigs were approved by the Institut Pasteur local ethic committee (CETEA).

Young conventional guinea pigs (3 weeks, female, Dunkin-Hartley, < 150g) were used for *Shigella* infection and hypoxia detection studies<sup>23</sup>. When indicated, neutropenia was generated in guinea pigs by two intraperitoneal injections of cyclophosphamide (100 mg/kg on day 7 and 50 mg/kg on day 1). *Shigella* infection was achieved by an intrarectal challenge of animals with 10<sup>10</sup> CFU exponentially grown. Infection proceeded for 8 hours before animals were sacrificed and the distal 10 cm of colon harvested and then flushed with 4% paraformaldehyde (PFA) in 1xPBS and inverted on wooden skewers. Tissues were kept in 4% PFA-1xPBS for 1- to 2-hours to complete fixation and then incubated in 1xPBS-glycine (100 mM) for 30 minutes to quench the PFA. Tissues were immersed successively in 15% and 30% sucrose at 4°C overnight and then released from the skewers by a longitudinal incision and prepared as swissrolls<sup>7</sup>. Swissrolls were embedded in Tissue-Tek OCT compound (Sakura) using a flash-freeze protocol and frozen at -80°C. For standard immunofluorescence staining, 10 µm sections were obtained using a cryostat CM-3050 (Leica). For hypoxia quantitative detection, 30 µm sections were generated.

Competitive Indexes were assessed and calculated *in vivo* on homogenized luminal and colonic mucosa bacteria content (M90T vs M90T *cydAB* mutant and BS176 vs BS176 *cydAB* mutant).

### Colonic tissue processing for Quantitative analysis

**Immunostaining**—For IF samples used for quantitative analyses, transversal colon sections of 30 µm thickness were stained using a modified protocol from Arena and colleagues<sup>24</sup>. Briefly, tissues on slides were fixed with 4% PFA for 10 minutes at room temperature. They were then washed with 1xPBS and stained using an α-EF5-Cy3 antibody solution (supplied by University of Pennsylvania) supplemented with 0.1% Triton, 1% BSA, and MUB<sub>40</sub>-Dylight405 (1 µg/mL) overnight at 4°C. The following day, the slides were washed with 1xPBS and mounted with ProLongGold® (Invitrogen).

**Imaging**—For quantification, fluorescence 3D images were acquired with an automated spinning-disk microscope (CellVoyager 1000, Yokogawa Electrics, Japan). The swissrolls were first scanned with a 10x air objective (Olympus, UPLSAPO 10x 0.4NA air) in bright-field to locate the tissue, followed by a scan to locate GFP-expressing *S. flexneri*. Infection

foci were imaged with a 40x oil objective (Olympus, UPLSAPO 40x 1.3NA oil) over 3 fluorescence channels (405, GFP, AF568) and bright field, capturing a 40  $\mu\text{m}$  thick section to encompass the whole tissue. Full fields made of 1x2 to 7x5 3D tiles of 200  $\mu\text{m}$   $\times$  200  $\mu\text{m}$   $\times$  40  $\mu\text{m}$  each were acquired depending on the size of the given site.

### Image Quantitative analysis

**Hypoxia profiles through colonic mucosa**—The lamina propria was delineated using Fiji<sup>25</sup>. Intensity profiles were generated from 10  $\mu\text{m}$  thick lines on maximum-intensity projections of the 3D images in the EF5 channel averaged with a Gaussian filter with  $\sigma = 10$   $\mu\text{m}$  (Figure 1a). The profiles ran into the tissue, orthogonally to the lamina propria, and their location was selected to traverse an infectious focus for infected tissues and randomly arranged for non-infected tissues.

The hypoxia curves of Figure 1b are generated by measuring several profiles that run through the LP from the apical surface to the basal surface (Figure 1a). Within one condition (infected or non-infected), all profiles are aligned with respect to the first local maximum (that crosses the LP surface). After alignment, we have the EF5 signal distribution - one value per profile - as a function of the tissue depth. We then compute the mean EF5 signal (thick line on Figure 1b) and its standard deviation (shaded area on Figure 1b) and report them as function of the tissue depth.

We then perform a Student t-test at each position along the tissue depth, comparing the distribution of EF5 signal at a given depth between profiles through tissues of infected (red) and non-infected (blue) animals, for all depths. We then report the range of depths for which this test reveals significant differences as black horizontal line over the plot. Figure 1b displays one of three repetitions. The infected and not-infected curves are made respectively of averaging 128 and 61 profiles. Sample size was adjusted to reach statistical differences between compared conditions. A blind analysis was used for image acquisition.

**Hypoxia measurements at single-cell level**—Automatic segmentation of individual *S. flexneri* and neutrophils was carried out using TrackMate<sup>26</sup>, yielding their X, Y, and Z coordinates and their local hypoxia levels measured from the EF5 channel averaged with a 3D Gaussian filter with  $\sigma = 2$   $\mu\text{m}$ . Together, bacterial and neutrophil positions and the manual annotations were processed using MATLAB (The MathWorks) for further analysis (Figure 2 and Figure 3).

We inspected infection foci manually and estimated their radius to be approximately 16  $\mu\text{m}$ . Clustered bacteria were therefore defined as bacteria that have at least 6 other bacteria in a neighborhood of 16  $\mu\text{m}$  in radius from their position (Supplementary Figure 1a). Isolated bacteria were defined as those having no other bacteria in a neighborhood of a 30  $\mu\text{m}$  radius from their position. Bacteria that did not fall into these two categories were not included in the analysis (Supplementary Table 1).

**Mean hypoxia spatial profile generated by bacteria**—The hypoxia profile around single-bacteria was calculated by averaging the EF5 signal (filtered with  $\sigma = 2$   $\mu\text{m}$ ) of all pixels at a fixed distance from the closest bacterium (Supplementary Figure 1b). Pixel

distance to the closest bacterium was calculated thanks to the image distance transform, taking into account the non-isotropy of the pixel size (0.2  $\mu\text{m}$ /pixel in XY and 1  $\mu\text{m}$ /pixel in Z). Locations outside of the tissue were not included in the profile. Pixels were then pooled in 1- $\mu\text{m}$  bins from 0 to 50  $\mu\text{m}$ . All the EF5 intensity of pixels in a single bin contribute to the mean and standard deviation at the bin distance and build the profiles of Supplementary Figure 2d. Single bins incorporated between 600 and 3.  $10^6$  measurements for a single image. This procedure was repeated on 16 images, treating separately clustered and dispersed bacteria. These hypoxia profiles average EF5 levels over all pixels at a specified distance, hereby canceling contributions from other potential sparse hypoxia sources such as neutrophils.

To investigate whether or not neutrophils contribute a significant addition to this hypoxia, we sought for each neutrophil the closest bacterium and categorized them as dispersed or clustered. We then reported on the hypoxia profile, the EF5 level, of the neutrophil at the measured distance to the closest bacterium, respectively, whether the closest bacterium was dispersed or clustered. A one-sided z-test was used to determine whether or not the neutrophil hypoxia could be explained by the bacteria hypoxia profile at this distance (dots) or if it was significantly larger (crosses, significance level at 5%). Less than 5% of neutrophils had a significantly higher hypoxia levels than what was generated by bacteria over 16 repetitions of this analysis.

**Bacteria and neutrophil density**—Whole tissue densities (Supplementary Figure 2a,c-d) were calculated by counting the number of neutrophils or bacteria, regardless of their clustering status, in the total tissue volume imaged for each experimental condition.

Clustered *Shigella* density (Figure 2d) was calculated by counting the number of neighbors in a sphere of radius 16  $\mu\text{m}$  around the 61119 clustered bacteria detected in the conventional animals, the M90T + EF5 condition. Dispersed *Shigella* density was calculated by counting the number of dispersed bacteria in the volume of the imaged tissue averaged over the 37 tissue sections of the same condition. Neutrophil density was calculated by counting the number of neutrophils in the volume of the imaged tissue averaged over a subset of 16 tissue sections of the same condition.

**T3SS activity reporter signal analysis**—We expressed the TSAR T3SS activity reporter<sup>2</sup> in *S. flexneri* wild-type strain; EF5 injected guinea pigs were infected with this strain as described above. The reporter emits in the Cyan channel (CFP) for all bacteria and in the Green channel for bacteria that are positive for T3 activity (fast-maturing eGFP, Rep+). GFP level corresponding to an active T3SS (Rep+) was determined *in vitro* by culturing *S. flexneri* 5a pTSAR in the presence or absence of oxygen, with or without congo red (0.01%). More than 100 individual bacteria were analyzed in each condition *in vitro*. We then imaged tissue sections, focusing on bacteria foci and proceeded to a similar analysis. We quantified signals in 2488 WT bacteria located in foci of infection.

## Statistical analysis

All statistical analyses have been performed with MATLAB software (The MathWorks). Comparisons with two groups (Figures 1b, 1h, 1i, 2b) were supported with Student

unpaired-*t* tests. Comparisons with three groups or more were supported by 1-way ANOVA test (Figures 1f, 3d, 3e, 4b and Supplementary Figures 4b,d-e) and 2-way ANOVA test (Figures 2g, 3b and Supplementary Figure 4c), followed by a *post hoc* Tukey test.

When *p*-values for the significance of pairwise comparisons were calculated (either from a Student-*t* test or a *post hoc* Tukey test after an ANOVA test) and displayed on figures, we used the following convention:

- *ns* not significant;  $p \geq 0.05$ ;
- \* $p < 0.05$  &  $p \geq 0.01$ ;
- \*\*  $p < 0.01$  &  $p \geq 0.001$ ;
- \*\*\*  $p < 0.001$ .

### Box-plots

When results are presented in the shape of a box-plot (Figures 1f, 1h, 1i, 2b), the central mark indicates the median, and the bottom and top edges of the box indicate the 25<sup>th</sup> and 75<sup>th</sup> percentiles, respectively. The whiskers extend to the most extreme data points not considered outliers, and the outliers are not plotted. Outliers are data points that are further away than 1.5 times the range from the 1<sup>st</sup> to the 3<sup>rd</sup> quartile, respectively above or below the 3<sup>rd</sup> and 1<sup>st</sup> quartile.

### Direct oxygen consumption quantification *in vitro*

Direct oxygen quantifications were performed in gas-proof glass punchable tubes (BD Vacutainer Z, reference 368430) using an oximeter (OXY-Meter, Unisense) combined with a needle sensor for piercing (OX-NP). Data was recorded using the SensorTrace logger software (Unisense). Glass tubes were first opened in an anaerobic cabinet (MiniMac DG250, Don Withley) for 30 min to ensure that all traces of exogenous oxygen were removed from the tube (anoxic atmosphere). Such conditioned tubes were subsequently filled with 2 mL of a culture medium (RPMI 1640 + 10 mM Hepes for neutrophils), pre-stabilized at 37°C and at  $pO_2 = 40$  mmHg (5%  $O_2$ ) in a hypoxic chamber (In vivo 500, Don withley) (Figure 2e). Prior to their inoculation, bacteria (*S. flexneri* 5a wild-type and mutant strains, *E. coli*, *S. typhimurium*, *L. monocytogenes*, *S. aureus* or *L. casei*) were grown in similar conditions until  $OD_{600} = 0.3$  was reached. Bacteria alone or with neutrophils were resuspended at the indicated concentrations in RPMI 1640 + 10 mM Hepes. When indicated Diphenyleiiodonium chloride (DPI, Sigma-Aldrich) was added at a 25  $\mu$ M final concentration, N-Formyl-Met-Leu-Phe (FmlF, Sigma-Aldrich) at 1  $\mu$ M. Direct oxygen quantification were performed over time and initiated immediately after bacteria or cell inoculation. Results were averaged from at least three independent measurements.

### Supplementary Material

Refer to Web version on PubMed Central for supplementary material.

## Acknowledgements

We acknowledge France-BioImaging infrastructure supported by the French National Research Agency (ANR-10-INBS-04, Imagopole, JYT), ANR JCJC 2017-17-CE15-0012 (BSM), and the European Research Council (ERC Grant n°232798: 2009-AdG HOMEOPITH, PJS). E.T.A. was a Pasteur Foundation and Pasteur-Roux Fellow.

## Data availability.

The datasets generated and/or analyzed during the current study are available from the corresponding author on reasonable request.

## References

1. Marteyn B, et al. Modulation of Shigella virulence in response to available oxygen in vivo. *Nature*. 2010; 465:355–358. [PubMed: 20436458]
2. Cramer T, et al. HIF-1alpha is essential for myeloid cell-mediated inflammation. *Cell*. 2003; 112:645–657. [PubMed: 12628185]
3. Peyssonnaud C, et al. HIF-1alpha expression regulates the bactericidal capacity of phagocytes. *J Clin Invest*. 2005; 115:1806–1815. [PubMed: 16007254]
4. Walmsley SR, et al. Hypoxia-induced neutrophil survival is mediated by HIF-1alpha-dependent NF-kappaB activity. *J Exp Med*. 2005; 201:105–115. [PubMed: 15630139]
5. Huether, SE, McCance, KL. *Understanding Pathophysiology*. Elsevier Health Sciences; 2015.
6. Karhausen J, et al. Epithelial hypoxia-inducible factor-1 is protective in murine experimental colitis. *J Clin Invest*. 2004; 114:1098–1106. [PubMed: 15489957]
7. Campbell EL, et al. Transmigrating Neutrophils Shape the Mucosal Microenvironment through Localized Oxygen Depletion to Influence Resolution of Inflammation. *Immunity*. 2014; doi: 10.1016/j.immuni.2013.11.020
8. Arena ET, Tinevez J-Y, Nigro G, Sansonetti PJ, Marteyn BS. The infectious hypoxia: Occurrence and causes during Shigella infection. *Microbes Infect*. 2017 Mar; 19(3):157–165. [PubMed: 27884799]
9. Ziemer LS, et al. Noninvasive imaging of tumor hypoxia in rats using the 2-nitroimidazole 18F-EF5. *Eur J Nucl Med Mol Imaging*. 2003; 30:259–266. [PubMed: 12552344]
10. Bumann D. Heterogeneous host-pathogen encounters: act locally, think globally. *Cell Host Microbe*. 2015; 17:13–19. [PubMed: 25590757]
11. Davis KM, Isberg RR. Defining heterogeneity within bacterial populations via single cell approaches. *Bioessays*. 2016; 38:782–790. [PubMed: 27273675]
12. Anderson MC, et al. MUB<sub>40</sub> Binds to Lactoferrin and Stands as a Specific Neutrophil Marker. *Cell Chem Biol*. 2018 Apr 19; 25(4):483–493. [PubMed: 29478905]
13. Sheridan WG, Lowndes RH, Young HL. Intraoperative tissue oximetry in the human gastrointestinal tract. *Am J Surg*. 1990; 159:314–319. [PubMed: 2305939]
14. Uden G, Trageser M. Oxygen regulated gene expression in Escherichia coli: control of anaerobic respiration by the FNR protein. *Antonie Van Leeuwenhoek*. 1991; 59:65–76. [PubMed: 1854188]
15. Way SS, Sallustio S, Magliozzo RS, Goldberg MB. Impact of either elevated or decreased levels of cytochrome bd expression on Shigella flexneri virulence. *J Bacteriol*. 1999; 181:1229–1237. [PubMed: 9973350]
16. Campbell-Valois F-X, et al. A fluorescent reporter reveals on/off regulation of the Shigella type III secretion apparatus during entry and cell-to-cell spread. *Cell Host Microbe*. 2014; 15:177–189. [PubMed: 24528864]
17. Davis KM, Mohammadi S, Isberg RR. Community behavior and spatial regulation within a bacterial microcolony in deep tissue sites serves to protect against host attack. *Cell Host Microbe*. 2015; 17:21–31. [PubMed: 25500192]
18. Hughes ER, et al. Microbial Respiration and Formate Oxidation as Metabolic Signatures of Inflammation-Associated Dysbiosis. *Cell Host Microbe*. 2017; 21:208–219. [PubMed: 28182951]

19. Nizet V, Johnson RS. Interdependence of hypoxic and innate immune responses. *Nat Rev Immunol.* 2009; 9:609–617. [PubMed: 19704417]
20. Taylor CT, Colgan SP. Regulation of immunity and inflammation by hypoxia in immunological niches. *Nat Rev Immunol.* 2017; 17:774–785. [PubMed: 28972206]
21. Light SH, et al. A flavin-based extracellular electron transfer mechanism in diverse Gram-positive bacteria. *Nature.* 2018; 562:140–144. [PubMed: 30209391]
22. Dejean L, Beauvoit B, Guérin B, Rigoulet M. Growth of the yeast *Saccharomyces cerevisiae* on a non-fermentable substrate: control of energetic yield by the amount of mitochondria. *Biochim Biophys Acta.* 2000; 1457:45–56. [PubMed: 10692549]
23. Monceaux V, et al. Anoxia and glucose supplementation preserve neutrophil viability and function. *Blood.* 2016; 128:993–1002. [PubMed: 27402974]
24. Arena ET, et al. Bioimage analysis of *Shigella* infection reveals targeting of colonic crypts. *Proc Natl Acad Sci USA.* 2015; 112:E3282–90. [PubMed: 26056271]
25. Schindelin J, et al. Fiji: an open-source platform for biological-image analysis. *Nat Methods.* 2012; 9:676–682. [PubMed: 22743772]
26. Tinevez JY, et al. TrackMate: an open and extensible platform for single-particle tracking. *Methods.* 2017; 115:80–90. [PubMed: 27713081]

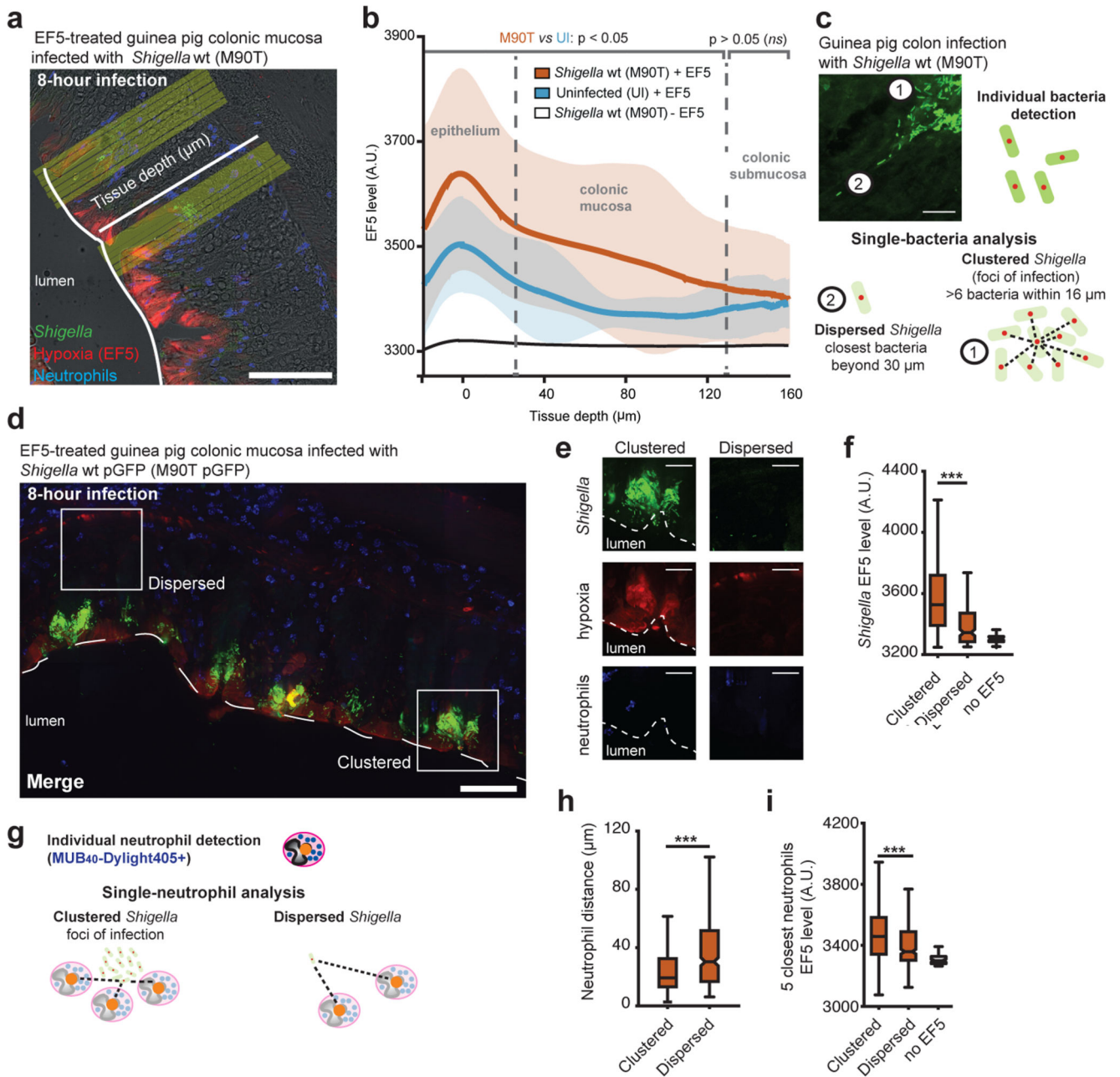


**Figure 1. Hypoxia is specifically induced by *Shigella* within foci of infection.**

**a.** Hypoxia was detected in guinea pig colonic mucosa infected with *S. flexneri* 5a pGFP strain (green) using the EF5 reporter<sup>9</sup>. EF5 was immunodetected with an a-EF5-Cy3 (red); neutrophils were labeled with the Myelotracker-Dylight405<sup>12</sup> marker (or Myelotracker-Alexa405<sup>12</sup>, blue). Scale bar: 50  $\mu\text{m}$ .

**b.** Hypoxia profiles through the colonic mucosa were reported. The EF5 level is reported as mean over all aligned profiles (thick lines)  $\pm$  standard deviation (shaded area) against tissue depth ( $n = 128, 61$  and  $48$  profiles averaged for respectively the M90T, uninfected and no-EF5 conditions). The gray segments atop the curves represent the range of depths for which

the EF5 levels are significantly different between the M90T and uninfected conditions (two-sided Student t-test,  $p < 0.05$ ).

**c.** Individual bacteria were detected by quantitative image analysis (red dot, see Supplementary Figure 1a), and two populations of *S. flexneri* were defined: as ‘dispersed’ if its closest neighbor was located beyond 30  $\mu\text{m}$  or as ‘clustered’ if at least 6 bacteria were within a 16  $\mu\text{m}$  diameter, forming a focus of infection. Scale bar: 20  $\mu\text{m}$ .

**d.** Detection of ‘clustered’ and ‘dispersed’ bacteria populations within the colonic mucosa. Scale bar: 50  $\mu\text{m}$ .

**e-f.** Hypoxia levels were compared at single ‘dispersed’ and ‘clustered’ bacteria levels by quantitative image analysis. Scale bar: 20  $\mu\text{m}$ . Hypoxia levels were significantly higher around ‘clustered’ compared to ‘dispersed’ bacteria (ANOVA 1-way test + Tukey test, on  $n = 61119, 186$  and  $11400$  bacteria, respectively for the clustered+EF5, dispersed+EF5 and no-EF5 conditions, see Supplementary Table 2). The no-EF5 signal was measured on infected tissues not stained with EF5.

**g.** Individual neutrophils (orange dot), stained with Myelotracker-Dylight405<sup>12</sup>, were localized in tissue by quantitative image analysis.

**h.** Neutrophils were found closer to ‘clustered’ bacteria compared to ‘dispersed’ bacteria (distance from  $n = 61119$  and  $186$  bacteria to the closest neutrophil for respectively the ‘clustered’ and ‘dispersed’ bacteria,  $p < 10^{-10}$ ).

**i.** The hypoxia level detected around neutrophils (averaged over the 5 closest) was higher around ‘clustered’ bacteria compared to ‘dispersed’ bacteria (EF5 levels around the 5 closest neutrophils, measured for  $n = 61119, 186$  and  $11400$  bacteria, respectively for the clustered+EF5, dispersed+EF5 and no-EF5 conditions,  $p \sim 10^{-10}$ ).

\*\*\* indicates  $p < 0.001$ . In the box-plots of panels f and h, the central mark indicates the median, and the bottom and top edges of the box indicate the 25th and 75th percentiles, respectively. The whiskers extend to the most extreme data points not considered outliers, and the outliers are not plotted. Outliers are data points that are further away than 1.5 times the range from the 1st to the 3rd quartile, respectively above or below the 3rd and 1st quartile.



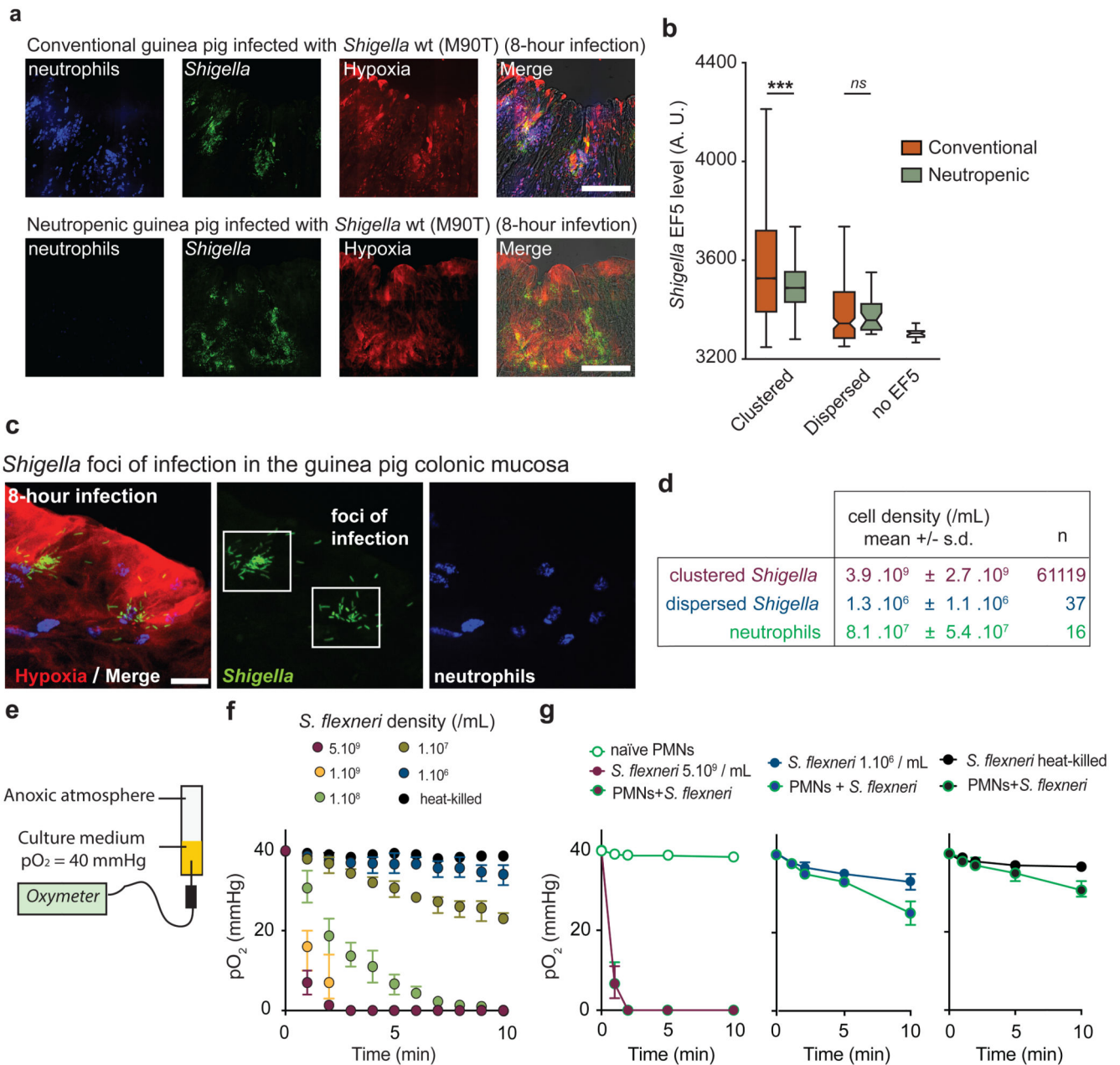


**Figure 2. Neutrophils are not essential for O<sub>2</sub> depletion in infected tissues, which is mainly caused by *Shigella* aerobic respiration.**

**a.** *S. flexneri* pGFP (green) foci of infection were detected in conventional (8 animals, 28 acquisitions) and neutropenic (3 animals, 7 acquisitions) guinea pig colonic mucosa.

Neutrophils were labeled with Myelotracker-Dylight405<sup>12</sup> (blue) and hypoxia with an  $\alpha$ -EF5-Cy3 (red). Scale bar: 50  $\mu$ m.

**b.** Hypoxia levels around ‘clustered’ bacteria were comparable between conventional vs neutropenic animals ( $p < 0.0001$ , see Supplementary Table 3).

**c-d.** Cell density of ‘clustered’ (in foci of infection) and ‘dispersed’ *S. flexneri* pGFP (green) populations were calculated *in vivo* (expressed as mean  $\pm$  S.D). Neutrophils were labeled

with Myelotracker-Dylight405<sup>12</sup> (blue) and hypoxic areas with an  $\alpha$ -EF5-Cy3 (red). Scale bar: 2  $\mu$ m. For clustered bacteria, the density is calculated as the number of bacteria around each clustered bacterium within 16  $\mu$ m for 61119 bacteria. For dispersed bacteria and neutrophils, the density is calculated as the number of dispersed bacteria ( $n = 37$  loci imaged), respectively neutrophils ( $n = 16$  loci imaged), divided by the imaged tissue volume.

**e.** O<sub>2</sub> consumption rates were assessed *in vitro* with an oximeter in a RPMI 1640 + 10 mM Hepes culture medium stabilized at 40 mmHg (hypoxic chamber) in tubes sealed under anoxic conditions (see Methods). Exponentially grown bacterial cultures were inoculated at the indicated concentration ( $t = 0$ ).

**f.** O<sub>2</sub> depletion rate was correlated with *S. flexneri* bacterial density. O<sub>2</sub> tensions (expressed as mean  $\pm$  S.D.) were assessed at indicated cell densities surrounding ‘clustered’ and ‘dispersed’ population densities calculated *in vivo* (see **d.**) or in the presence of  $5.10^9$  heat-killed *S. flexneri* ( $n = 3$  independent experiments).

**g.** O<sub>2</sub> depletion rate (O<sub>2</sub> tensions expressed as mean  $\pm$  S.D.,  $n = 3$  independent experiments) in the presence of *S. flexneri* and neutrophils (PMNs,  $8.10^7$  neutrophils/mL). In the presence of  $1.10^6$  *S. flexneri*/mL or  $5.10^9$  heat-killed *S. flexneri*/mL, anoxia was not reached over the measurement period, although neutrophil O<sub>2</sub>-consumption was observed (10 min, see Supplementary Table 4).

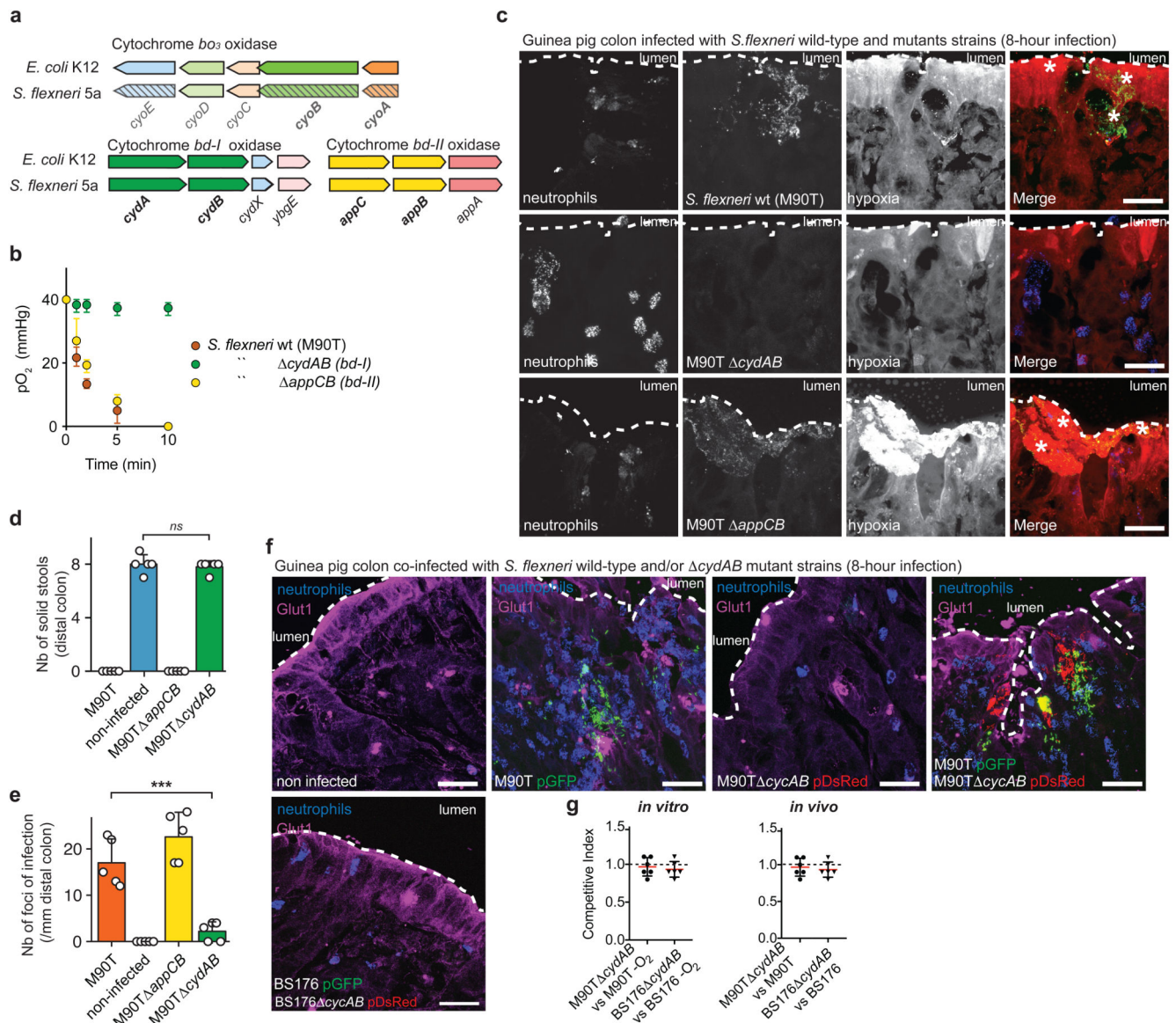


**Figure 3. Aerobic respiration is required for hypoxia induction and efficient colonic mucosa colonization by *Shigella* in vivo.**

**a.** Genetic organization of cytochrome oxidases (*bo<sub>3</sub>*, *bd-I* and *bd-II*) encoding genes in *Escherichia coli* K12 and *Shigella flexneri* 5a. *cyoA* and *cyoB* genes are not functional in *S. flexneri* due to genetic insertions.

**b.** *S. flexneri* 5a  $\Delta cydAB$  (*bd-I*) was unable to consume  $O_2$  *in vitro* in a RPMI 1640 + 10 mM HEPES medium stabilized at a  $pO_2 = 40$  mmHg and had a growth defect in the presence of  $O_2$  ( $n = 3$  independent experiments,  $p < 10^{-8}$ , 2-way ANOVA test, see Supplementary Figure 4c and Supplementary Table 5).  $O_2$  tensions expressed as mean  $\pm$  S.D.

**c.** *S. flexneri* 5a  $\Delta cydAB$  (*bd-I*) pGFP (green) was avirulent *in vivo* compared to wild-type and  $\Delta appCB$  (*bd-II*) mutant strains. Hypoxia was detected with a-EF5-Cy3 (red), neutrophils with Myelotracker-Dylight405<sup>12</sup> (blue). Scale bar: 50  $\mu$ m. This experiment was repeated independently three times with similar results.

- d.** Tissues infected with the *cydAB* strain were not inflamed as compared to the wild-type strain, as indicated by the presence of solid stools in the colon lumen (mean  $\pm$  S.D.,  $p > 0.8$ , see Supplementary Table 6).
- e.** The number of foci of infection was significantly reduced in tissues infected by the *cydAB* strain compared to the wild-type strain (mean  $\pm$  S.D.,  $p < 10^{-4}$ , see Supplementary Table 7).
- f.** GLUT-1 was detected with a monoclonal antibody (magenta) within *S. flexneri* 5a pGFP (green) hypoxic foci of infection. *S. flexneri* 5a *cydAB* pDsRed (red) was able to colonize the colonic mucosa upon co-infection with the wild-type strain (*S. flexneri* 5a pGFP). Plasmid-cured BS176 and BS176 *cydAB* remain in the luminal compartment. Neutrophils were labeled with Myelotracker-Dylight405<sup>12</sup> (blue). Scale bar: 70  $\mu$ m. See Supplementary Figure 5 for extended imaging. This experiment was repeated independently three times with similar results.
- g.** M90T/M90T *cydAB* and BS176/BS176 *cydAB* Competitive Indexes were determined in co-cultures *in vitro* ( $-O_2$  conditions) and upon guinea pig co-infection *in vivo* (lumen and colonic mucosa). CI=1 means no growth difference (mean  $\pm$  S.D., n=5 biologically independent animal samples). \*\*\* indicates  $p < 0.001$ .

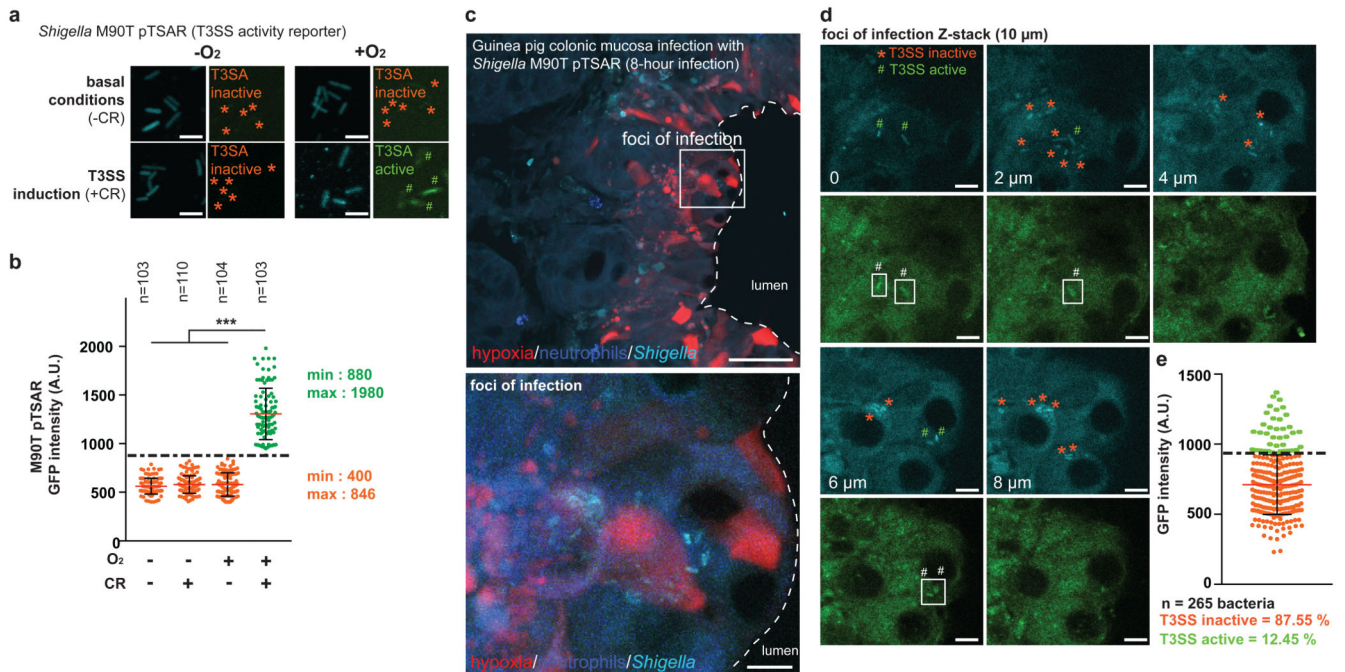


**Figure 4. *S. flexneri* T3SS is inactive in the colonic mucosa, supporting foci of infection extension.**

**a-b.** O<sub>2</sub>-dependent modulation of *S. flexneri* Type III secretion system (T3SS)<sup>1</sup> was confirmed *in vitro* in the presence of congo red (0.01%) using the activity reporter pTSAR<sup>16</sup> (bacteria are constitutively cyan (CFP); bacteria with an active T3SS have a high pTSAR signal (eGFP, green, #), not bacteria with an inactive T3SS (\*)); T3SS was active at a GFP signal intensity above 900 AU, as indicated by a 1-way ANOVA test (see Supplementary Table 8, \*\*\* indicates  $p < 0.001$ . Red lines and black bars: mean  $\pm$  standard deviation.)

**c.** T3SS activity was assessed at a single-bacteria level *in vivo*, in hypoxic foci of infection formed by *S. flexneri* pTSAR. This experiment was repeated independently three times with similar results.

**d-e.** Bacteria with an active T3SS are indicated in the green channel (#) in Z-stack image series, and bacteria with an inactive T3SS are indicated in the cyan channel (\*). Most of *S. flexneri* pTSAR individual bacteria detected within hypoxic foci of infection have an inactive T3SS (\*, 87.66% total population with eGFP signal intensity above 900 AU,  $n = 286$  bacteria. Red and black bars are mean  $\pm$  S.D.  $n = 3$  biologically independent animal samples).